Biochimie 94 (2012) 516–524

Contents lists available at SciVerse ScienceDirect

Biochimie

journal homepage: www.elsevier.com/locate/biochi

Research paper

Catalytic and regulatory roles of divalent metal cations on the phosphoryl-transfer mechanism of ADP-dependent sugar kinases from hyperthermophilic archaea

Felipe Merino[1], Jaime Andrés Rivas-Pardo[1], Andrés Caniuguir, Ivonne García, Victoria Guixé*

Laboratorio de Bioquímica y Biología Molecular, Departamento de Biología, Facultad de Ciencias, Universidad de Chile, Las Palmeras 3425, Casilla 653, Santiago, Chile

ARTICLE INFO

Article history:
Received 21 May 2011
Accepted 29 August 2011
Available online 2 September 2011

Keywords:
ADP-dependent kinase
Embden-Meyerhof pathway
Divalent metal cation
Enzyme inhibition

ABSTRACT

In some archaea, glucose degradation proceeds through a modified version of the Embden-Meyerhof pathway where glucose and fructose-6-P phosphorylation is carried out by kinases that use ADP as the phosphoryl donor. Unlike their ATP-dependent counterparts these enzymes have been reported as non-regulated. Based on the three dimensional structure determination of several ADP-dependent kinases they can be classified as members of the ribokinase superfamily. In this work, we have studied the role of divalent metal cations on the catalysis and regulation of ADP-dependent glucokinases and phosphofructokinase from hyperthermophilic archaea by means of initial velocity assays as well as molecular dynamics simulations. The results show that a divalent cation is strictly necessary for the activity of these enzymes and they strongly suggest that the true substrate is the metal-nucleotide complex. Also, these enzymes are promiscuous in relation to their metal usage where the only considerations for metal assisted catalysis seem to be related to the ionic radii and coordination geometry of the cations.

Molecular dynamics simulations strongly suggest that this metal is bound to the highly conserved NXXE motif, which constitutes one of the signatures of the ribokinase superfamily. Although free ADP cannot act as a phosphoryl donor it still can bind to these enzymes with a reduced affinity, stressing the importance of the metal in the proper binding of the nucleotide at the active site. Also, data show that the binding of a second metal to these enzymes produces a complex with a reduced catalytic constant. On the basis of these findings and considering evolutionary information for the ribokinase superfamily, we propose that the regulatory metal acts by modulating the energy difference between the protein-substrates complex and the reaction transition state, which could constitute a general mechanism for the metal regulation of the enzymes that belong this superfamily.

1. Introduction

For some archaea the glucose degradation proceeds through a modified version of the Embden-Meyerhof pathway where the phosphorylation of glucose and fructose-6-P is performed by kinases that use ADP instead of ATP as phosphoryl donor [1]. Generally, these enzymes are found in hyperthermophilic and methanogenic archaea belonging to the *thermococcales*, *methanococcales*, and *methanosarcinales* orders [2–5], but also an ADP-dependent glucokinase in *Mus musculus* has been reported [6]. These kinases are homologous to each other and they do not show sequence identity, over the noise level, with any of the hitherto known ATP-dependent kinases. However, despite the lack of sequence identity with other enzymes, the three dimensional structure determinations of several ADP-dependent kinases have allowed to classify them as members of the ribokinase superfamily [7]. Besides ADP-dependent kinases, the ribokinase superfamily includes ATP-dependent kinases of adenosine, fructose, tagatose-6-P, fructose-6-P, fructose-1-P, ribose, and pyridoxal amongst others [8]. Structurally, these proteins have a Rossman-like fold, with a central β-sheet composed of mainly parallel strands and eight α-helices, five in one side and three on the other, which is known as the large domain [9]. Besides this core ribokinase-like fold, some of the members of the superfamily present a smaller domain composed of four to five strands and occasionally some helices.

Abbreviations: EPR, Electronic paramagnetic resonance; MeADP, metal-ADP complex; ADP-GK, ADP-dependent glucokinase; ADP-PFK, ADP-dependent phosphofructokinase; *tl*GK, ADP-dependent glucokinase from *Thermococcus litoralis*; *pf*GK, ADP-dependent glucokinase from *Pyrococcus furiosus*; *ph*PFK, ADP-dependent phosphofructokinase from *Pyrococcus horikoshii*; Pfk-2, Phosphofructokinase-2 from *Escherichia coli*.

* Corresponding author. Tel.: +56 2 9787335; fax: +56 2 2712983.
E-mail address: vguixe@uchile.cl (V. Guixé).

[1] These authors contributed equally to this work.

0300-9084/$ – see front matter © 2011 Elsevier Masson SAS. All rights reserved.
doi:10.1016/j.biochi.2011.08.021

Unlike most phosphofructokinases and glucokinases, the members of the ADP-dependent sugar kinase family have been described as non-regulated enzymes given that they present hyperbolic saturation kinetics for both of their substrates [2,3,5] and no allosteric effectors have been reported to date [10]. For ADP-dependent phosphofructokinases, this seems to be a key difference with respect to their ATP-dependent counterparts since it has been previously shown that MgATP inhibition, a feature shared by prokaryotic and eukaryotic enzymes, is a necessary regulation mechanism to avoid net ATP hydrolysis [11]. In spite of this, there is preliminary evidence that some of the ADP-dependent kinases are inhibited by high concentrations of divalent metal cations [10].

Structural based sequence alignments of several members of the ribokinase superfamily have revealed two highly conserved motifs related with the common catalytic mechanism of these enzymes. A strictly conserved aspartic acid residue, inside a motif called GXGD, is proposed to act as the catalytic base that removes the proton from the acceptor hydroxyl group thus activating it for the nucleophilic attack [12–16]. Mutation of this residue leads to enzymes with catalytic constants up to three orders of magnitude lower than the wild type versions [12,16–19].

On the other hand, two highly conserved residues, aparagine and glutamic acid, inside a motif called NXXE are believed to be involved in metal binding [20,21]. Crystallographic structures of some ATP-dependent members of the superfamily have revealed that this motif is involved in the coordination of the divalent metal cation located between the γ and β-phosphates of the nucleotide [22–24]. Interestingly, the structure of adenosine kinase from *Homo sapiens* presents a magnesium ion in this position even when there is no phosphate present [13]. Additionally, in some structures, a second ion bound to the phosphates of the nucleotide has been observed [22–24]. On the basis of enzymatic measurements, it has been demonstrated that the activity of some members of the ribokinase superfamily is strongly dependent on the amount of free divalent metal cation present. However, the kinetic effect elicited by the free metal is strictly related to the enzyme assayed. For example, while adenosine kinases from different sources are inhibited by high concentrations of magnesium [20], the phosphofructokinase-2 (Pfk-2) from *Escherichia coli* is activated by it [21,25]. Then, the kinetic measurements are also pointing towards the presence of a second metal binding site in these enzymes, which suggests that the second ion observed in the crystallographic structures is kinetically relevant. Even though the kinetic behavior of different members of the ribokinase superfamily against free metal concentration shows opposite trends, mutation of the glutamic acid inside the NXXE motif on either adenosine kinase [20] or phosphofructokinase-2 [21,25] affects the catalytic constant (k_{cat}) of the enzymes as well as the regulatory properties elicited by the metal, suggesting that the catalytic and regulatory metal binding sites are structurally coupled.

Even when the above data highlight the role of metals in the catalytic mechanism of the ribokinase superfamily members, there are no studies regarding the kinetic aspects of these effectors on the catalytic mechanism of the ADP-dependent kinases which are, by far, the less studied enzymes of the superfamily. Unfortunately, while there are several members of the ADP-dependent sugar kinase family with known crystallographic structures [7,17,18,26], none of them show a divalent metal cation bound, which hinders the possibility of making any structure based hypothesis regarding activity regulation by metals in these enzymes.

In this work we propose that the activity of ADP-dependent kinases is regulated by divalent metal cations due to binding of this ligand to a second site. To test this hypothesis we analyzed the influence of them on the activity of the ADP-dependent glucokinase from *Pyrococcus furiosus* (*pf*GK), the ADP-dependent glucokinase from *Thermococcus litoralis* (*tl*GK), and the ADP-dependent phosphofructokinase from *Pyrococcus horikoshii* (*ph*PFK) by means of kinetic assays as well as molecular modeling and molecular dynamics calculations. The results show that a complex between a divalent metal cation and the nucleotide is required for the phosphoryl transfer reaction. Also, the data suggest the presence of a second metal binding site which regulates the activity by producing an enzyme with a reduced catalytic constant. Finally, the molecular dynamics simulations strongly suggest that the metal bound to the NXXE motif is the catalytic one. On the basis of these findings an inhibitory mechanism is proposed which can be applied to the regulation of other members of the ribokinase superfamily.

2. Materials and methods

2.1. Expression and purification of the ADP-dependent enzymes

The *tl*GK and the *pf*GK genes were over-expressed in the *E. coli* strain BL21 (DE3) pLysS using the expression vector pET-17b. Cells were cultured at 37 °C in Luria Bertani broth containing 100 μg/mL ampicillin and 35 μg/mL chloramphenicol until the OD_{600} reached ~0.4 when Isopropyl-β-D-thiogalactopyranoside was added to a final concentration of 1 mM to induce expression over night. Cells were harvested by centrifugation, resuspended in TrisHCl 100 mM, 5 mM $MgCl_2$, pH 7.8 (Buffer A), and disrupted by sonication. The crude extract was incubated at 90 °C for 30 min, and the denatured protein was then removed by centrifugation (8230 g). Then the solution was saturated with 60% $(NH_4)_2SO_4$ and incubated for 1 h at 4 °C. The precipitated protein was removed by centrifugation (8230 g). The soluble part was loaded into a t-butyl HIC Cartridges (BioRad, 5 mL). Protein was eluted with a lineal gradient of $(NH_4)_2SO_4$ (from 60 to 0%). The active fractions were pooled, dialyzed against buffer A, and loaded in DEAE-cellulose (for *pf*GK) or a MonoQ HR 5/5 (Pharmacia) (for *tl*GK) column and eluted with a lineal gradient of KCl (0–1 M). The active fractions were pooled, dialyzed against buffer A, concentrated, and used as the purified enzyme preparation. *ph*PFK was expressed and purified essentially as described in [18], but replacing the single elution step with 0.5 M imidazole by a gradient between 20 and 500 mM imidazole and removing the size exclusion chromatography step.

2.2. Kinetics studies

All kinetic experiments were performed on a Hewlett Packard 8453 spectrophotometer. *ph*PFK activity was assayed at 50 °C, by coupling the fructose-1,6-bisP formation to the oxidation of NADH. The *ph*PFK solution was mixed with a reaction mixture containing 25 mM PIPES buffer, pH 6.5, fructose 6-P, ADP and divalent metal as indicated, 0.2 mM NADH, 1.96 U α-glycerophosphate dehydrogenase, 19.6 U triosephosphate isomerase, and 0.52 U aldolase (all enzymes were from rabbit muscle). *pf*GK and *tl*GK activities were assayed spectrophotometrically at 40 °C, by coupling the glucose-6-P formation to the reduction of NAD^+. Glucokinase preparations were mixed with a reaction buffer containing 50 mM HEPES, pH 7.8, glucose, ADP, and divalent metal as indicated, 0.5 mM NAD^+, and 1.4 units of glucose-6-P dehydrogenase from *Leuconostoc mesenteroides*. The change in NADH concentration was followed spectrophotometrically at 340 nm using and extinction coefficient of 6.22 mM^{-1} cm^{-1} [27].

Kinetics parameters were obtained by measuring enzyme activities as a function of the concentration the metal-ADP complex (MeADP), while keeping the concentrations of fructose 6-P or glucose at fixed saturating levels. The concentration of free metal was held constant at 1 mM. In all kinetics studies, the concentrations

of free divalent metal, ADP^{3-}, and $MeADP^{1-}$ were calculated from the total concentration of the nucleotide-(ADP_t) and divalent cation used in the assay, assuming a dissociation constant of 676 μM for Mg^{2+}, 66 μM for Co^{2+}, and 93 μM for Mn^{2+} in the equilibrium $MeADP^{1-} \leftrightarrow ADP^{3-} + Me^{2+}$. The dissociation constants were obtained from the Critical Metal Complexes Database Version 5.0 (Texas A&M University). The experimental curves were fitted using Sigmaplot 11.0 software (Systat Software, Inc.).

The metal specificity of the ADP-dependent enzymes was tested by measuring the activity as described above using $MgCl_2$, $MnCl_2$, $NiSO_4$, $CoCl_2$, or $CaCl_2$ and an excess of 1 mM of metal over the ADP concentration.

For each assay, control experiments were performed to discard any specific or unspecific effect of the divalent metals on the activity of the coupled enzymes.

2.3. Models for metal inhibition mechanism

Competitive, partial and total uncompetitive and mixed mechanism were tested for the cation induced inhibition of *tl*GK, *ph*PFK, and *pf*GK by performing global fits of saturation curves at different concentrations of free metal using the Sigmaplot 11.0 software (Systat Software, Inc.).

2.4. Electronic paramagnetic resonance spectroscopy

Mn^{2+} binding to *tl*GK was measured by means of electronic paramagnetic resonance (EPR) spectroscopy essentially as described in [25], but using a fixed concentration of Mn^{2+} of 50 μM and varying the protein concentration between 0 and 500 μM. All measurements were performed at 40 °C.

2.5. Molecular simulations

Langevin dynamics simulations were performed with NAMD 2.7 [28] using the CHARMM27 force field [29]. Initial structures were obtained as follows: for glucokinases the x-ray structure of *pf*GK in presence of AMP and glucose was used starting point [17]. The extra phosphate was incorporated to AMP to produce ADP and a water molecule close to the position where the NXXE cation must be located was transformed into magnesium. Indeed, the cluster of water molecules present there has already been suggested as a possible binding site for this ion [17]. Moreover, Ito et al. [7] have seen a zone of unexplained electron density in the structure of the glucokinase from *T. litoralis* near the NXXE motif which they attributed to the presence of magnesium ion. However, given that it does not shown the typical octahedral geometry it was not assigned to the metal in the final structure. For *ph*PFK the model was essentially constructed as it was done for the bifunctional enzyme from *Methanocaldococcus jannaschii* as described before [30]. The initial position of MgADP (including the magnesium coordination sphere) was inferred from the resulting structure for *pfGK*.

The systems were softly thermalized after minimization between 50 and 320 K increasing the temperature by 10 K every 2 ps. After that, the system was equilibrating using Langevin dynamics to complete 2 ns. Later, the system was simulated for another 3 ns. Temperature and pressure were targeted to a value of 320 K and 1 bar respectively. The r-RESPA integrator was used with a 2 fs timestep for short range forces and 4 fs for long range forces. All bonds involving hydrogen atoms were restricted to their equilibrium length. The proteins were putted in a box of water with an extension of 1.2 nm far from the last protein atom in each direction and periodic boundary condition was used. The systems were neutralized with NaCl to a final concentration of 0.1 M.

For simulations in the absence of divalent cation, magnesium was removed from the last frame of the corresponding simulation and a protocol essentially as the one described above was used. All images were prepared using VMD [31].

3. Results and discussion

3.1. Role of the divalent metal cations in the catalysis of the ADP-dependent phosphofructokinase and glucokinases

To understand the role that divalent metal cations play in the catalytic mechanism of enzymes that belong to the ADP-dependent sugar kinase family, we used as experimental models the ADP-dependent glucokinase from *T. litoralis*, the ADP-dependent glucokinase from *P. furiosus*, and the ADP-dependent phosphofructokinase from *P. horikoshii* since for these enzymes the three dimensional structure is known at atomic resolution and allow us to use a multidisciplinary approach that includes initial velocity studies, molecular modeling and molecular dynamics calculations.

Many phosphoryl transfer enzymes require a divalent metal cation for their activity [32]. The role of metals in catalysis may be ligand binding and therefore forming the true substrate or alternatively metal can bind directly to the enzyme and alter its structure and/or serve a catalytic role [32]. To test whether different divalent metals cations are able to support the ADP-dependent kinase activity, the reaction velocity was measured in the presence of Mg^{2+}, Mn^{2+}, Ni^{2+}, Co^{2+}, or Ca^{2+} as the unique metal present. Fig. 1 shows the measured activity, relative to the velocity obtained in the presence of magnesium, for the three enzymes. *ph*PFK is able to use any of the assayed metals, showing the highest activity in the presence of cobalt. On the other hand, both glucokinases show the highest activity in the presence of magnesium, manganese, or cobalt. Nickel can also be used by these two proteins, but the velocity obtained in this case represents only a 25% for *pf*GK and 40% for *tl*GK of the one obtained in the presence of Mg^{2+}. Noticeably, *ph*PFK can use also calcium and nickel to support the

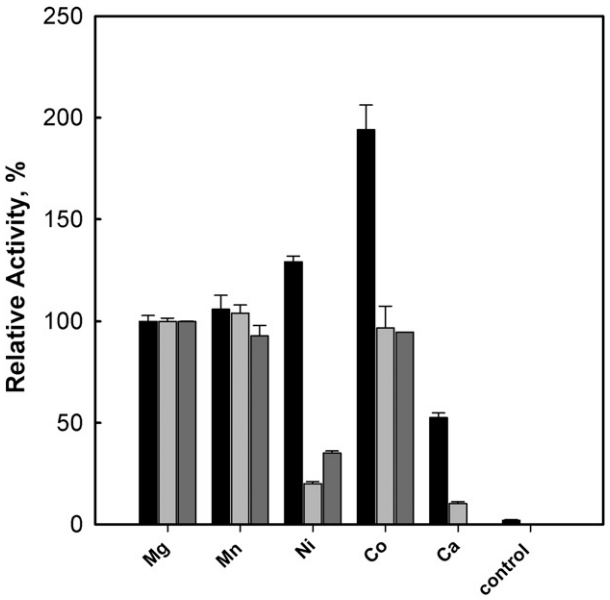

Fig. 1. Metal especificity of the ADP-dependent enzymes. Black bars correspond to phosphofructokinase from *Pyrococcus horikoshii*, clear gray bars correspond to glucokinase from *Thermococcus litoralis*, and dark gray bars correspond to glucokinase from *Pyrococcus furiosus*. The assays were performed with an excess of 1 mM divalent metal over the ADP concentration. The results are relative to the activity measured in the presence of Mg^{2+}. Controls were performed in the absence of metal and in presence of EDTA.

enzymatic activity being, in terms of metal usage, the most promiscuous of the three ADP-dependent enzymes. Also, none of the ADP-dependent enzymes assayed showed activity when the assay was performed in the presence of EDTA, which strongly suggests that the true substrate is the nucleotide-metal complex. As a general trend, the highest activities were obtained in the presence of Mg^{2+}, Mn^{2+}, and Co^{2+}. For this reason, the kinetic parameters for these metals in complex with ADP were determined.

Table 1, summarizes the result of these experiments. For all the enzymes, the K_m values for the three metal-nucleotide complexes tested are very similar. In the most extreme case (*ph*PFK) the variation of K_m values for different metal-complexes is at most three-fold when the K_m value for CoADP is compared to the ones obtained for MnADP or MgADP. This suggests that the affinity for the metal-nucleotide complex is somehow independent of the metal identity.

In terms of k_{cat}, cobalt is the best metal for *ph*PFK and *tl*GK. For *pf*GK the k_{cat} values for either MnADP or CoADP are statistically equal while, on the other hand, these two are slightly higher than the k_{cat} obtained for MgADP (Table 1). In order to assess the catalytic efficiency of these enzymes with respect to the metals assayed, we calculate the k_{cat}/K_m parameter. In the case of *ph*PFK, the highest k_{cat}/K_m values were obtained for the Mg^{2+} and Mn^{2+} nucleotide complexes with no statistical difference between them. For *tl*GK, the metal-nucleotide complex with the highest k_{cat}/K_m value is CoADP, and for *pf*GK is MgADP. Nevertheless, the k_{cat}/K_m values for the three enzymes with all the metals tested are within the same order of magnitude, and the difference between them is at most 2-fold.

The use of Mg^{2+} and Mn^{2+} by these enzymes is not surprising since magnesium ions are, by far, the most used metals for phosphotransferase reactions either for electrostatic stabilization of charged species or to activate the substrates by polarizing C—O or P—O bonds [32]. Also, it has been documented that for many enzymes magnesium can be replaced by manganese where MgATP is used as a substrate [33]. On the other hand, cobalt is generally related to B12 dependent enzymes where it acts as a redox active center [32] and in fact, its use in phosphotransferase reactions is quite uncommon. Indeed, it has been proposed that the occurrence of cobalt in enzymes other than those related with B12, may be restricted to those that are evolutionary relics of the early phases of life [32]. However, this may not be our case since it has been proposed that the ADP-dependent enzymes are the most recent members of the superfamily [9].

Taken together, the results show that the ADP-dependent enzymes are promiscuous in relation to their metal usage where the only considerations for metal assisted catalysis seem to be related to the ionic radii and coordination geometry of the cations.

To evaluate the importance of the metal in the nucleotide binding to the active site, we performed kinetic studies regarding the inhibitory effect of free ADP on the reaction velocity when MgADP is the variable substrate. In fact, for many kinases, including Pfk-2 from *E. coli*, the free nucleotide can act as a very strong competitive inhibitor [34]. The results obtained for the three enzymes were globally fitted to a competitive inhibition model and the kinetic constants are summarized in Table 2.

The highest K_i value for free ADP was obtained for *ph*PFK (3.4 mM) while for *pf*GK and *tl*GK these values were 0.58 and 0.3 mM, respectively. The dissociation constant for free ADP is approximately two orders of magnitude higher than the K_m value[2] for MgADP in glucokinases and three orders of magnitude higher for the phosphofructokinase enzyme. These results demonstrate that free ADP behaves as a weak competitive inhibitor and highlight the importance of the metal in the proper binding of the nucleotide at the active site of the ADP-dependent enzymes. Importantly, this fact together with the observation that a metal divalent cation is strictly needed for catalysis, supports the idea that the metal-nucleotide complex is the true substrate of these enzymes.

3.2. Regulation of enzyme activity by divalent metal cations in the ADP-dependent phosphofructokinase and glucokinases

To further investigate the role of the divalent metal cations in the catalytic mechanism of these enzymes, the effect of increasing concentrations of free Mg^{2+}, Mn^{2+}, and Co^{2+}, measured at saturating conditions of substrates, was assayed. Fig. 2 shows the metal which has the largest effect on each enzyme. In the case of *ph*PFK, Mg^{2+} produces a decrease in the activity upon increasing the free metal concentration which reaches approximately an 85% of the activity measured at the lowest concentration of free cation assayed (60 μM). On the other hand Mn^{2+} is the metal with the highest inhibitory effect for both glucokinases. In this case, the cation decreases the reaction velocity to a value of 50% of the activity measured at the lowest concentration of free metal assayed (80 μM). It is important to stress out that for this kind of experiments due to the finite value of the dissociation constant for the formation of the metal-nucleotide complex it is impossible to perform experiments where the concentration of the free metal is zero.

Taking into account that only glucokinases are inhibited in a significant degree by the free metal, we investigated the mechanism of this inhibition by studying the effect of different free manganese concentrations on the kinetic parameters for *tl*GK and *pf*GK. The resulting curves were globally fitted to competitive and both partial and total mixed and uncompetitive inhibitory mechanisms. The analysis suggests that the inhibition of *tl*GK corresponds to a mixed mechanism where the inhibited form has no activity, while *pf*GK is inhibited according to a non-competitive mechanism, where the inhibited form has about half of the activity of the non-inhibited form. The results are summarized in Table 3.

Although the data are well adjusted to the proposed mechanism it has to be considered that for *tl*GK data from Fig. 2 suggest a partial and not a total mechanism. A mixed mechanism contains two binding steps: one between the effector (the metal in this case) and the free protein and one between the effector and the protein substrate complex (here MeADP-enzyme). To test the model and the apparent discrepancy between the global fit and the experimental data, we compared the value of some of the predicted constants with one determined experimentally. Because of its value as a paramagnetic probe, we evaluate the manganese binding to the free protein by electronic paramagnetic resonance spectroscopy. Experiments performed with *tl*GK showed that manganese can indeed bind to the free enzyme, but with a dissociation constant of 58 ± 9 μM (Fig. 3) and a stoichiometry of 1.1 ± 0.2. This K_d value is far from the value of 1.2 mM estimated from the global fit to a mixed mechanism, which stress the importance of evaluating the validity of the adjusted parameters against experimental data. Taken together, these considerations prompted us to reassess the metal inhibition mechanism of these enzymes.

High resolution structures of several ATP-dependent members of the ribokinase superfamily show two cations at the active site [22–24]. The first one is always bound to the nucleotide and to the NXXE motif. This sequence motif is also present in the ADP-dependent sugar kinase family (Fig. 4). The position of the second

[2] Here we are referring to the K_m value calculated from the fit in Table 2 since this represents the constant in the absence of free ADP. Given that it is not possible to do this experimentally, the value is a little lower than the one measured directly.

Table 1
Kinetic parameters of the ADP-dependent enzymes using MeADP as the varying substrate complexed with different divalent metal cations. All experiments were performed using a free metal concentration of 1 mM.

	*ph*PFK			*tl*GK			*pf*GK		
	K_M μM	k_{cat} s^{-1}	k_{cat}/K_M s^{-1} μM^{-1}	K_M μM	k_{cat} s^{-1}	k_{cat}/K_M s^{-1} μM^{-1}	K_M μM	k_{cat} s^{-1}	k_{cat}/K_M s^{-1} μM^{-1}
Mg^{2+}	8 ± 2	52 ± 4	6.5 ± 1.7	23 ± 0.2	35 ± 0.3	1.5 ± 0.018	14 ± 2	104 ± 3	7.4 ± 1.1
Mn^{2+}	8 ± 1	67 ± 4	8.4 ± 1.2	17 ± 1	21 ± 0.4	1.2 ± 0.076	22 ± 1	116 ± 2	5.3 ± 0.26
Co^{2+}	22 ± 1	98 ± 5	4.4 ± 0.30	15 ± 0.2	44 ± 1	2.9 ± 0.077	25 ± 1	114 ± 3	4.6 ± 0.22

one is variable, but it is always bound to the nucleotide, either to the α, β, or γ-phosphate. Mutagenic studies performed on the NXXE residues of Pfk-2 [21,25] and adenosine kinase [20] have produced enzymes with the catalytic and the regulatory properties altered, making it difficult to assign a regulatory or a catalytic role to one of these two metals. However, since in evolutionary terms the most conserved feature should be the catalytic mechanism, one can assume that the NXXE motif is most likely related to the binding of the catalytic metal. In this light, considering that the non-NXXE cation is the regulatory one, and given that the binding site of this metal is almost completely formed by the nucleotide, the general regulatory mechanism in the superfamily should be sequential, where the binding of nucleotide-metal complex is needed for the binding of the regulatory metal. For these reasons, we think that while the mixed mechanisms are able to numerically reproduce the inhibitory profiles, they are not describing the true regulatory mechanism of these enzymes and that the interaction between the metal and the free enzyme determined by EPR corresponds to binding of the catalytic metal. In fact, the structure of the human adenosine kinase shows a magnesium ion bound to the NXXE residues even in the absence of ATP supporting the idea that this metal corresponds to the catalytic one [13]. This idea is also reinforced by manganese binding experiments performed with the wild type Pfk-2 and with a mutant of the NXXE motif (E190Q) which reveals that the E190Q mutation does not affect the binding of neither the metal-ATP complex nor the activating metal, suggesting that the role of this residue is most likely linked to the stabilization of the transition state of the phosphoryl transfer reaction [25].

Since there is no information about the general kinetic mechanism of both glucokinases, which would be required to study the detailed inhibition mechanism for these enzymes and considering that the K_m values for the metal-nucleotide complex are not significantly affected by the concentration of free metal, we decided to focus on the effect of the free metal on k_{cat}. Let us consider a mechanism such as the one depicted in the Scheme 1 below.

There, ES represent the ternary complex between the enzyme and its substrates, ESI the ternary complex in the presence of the second cation, and $ES^{\ddagger}$ or $ESI^{\ddagger}$ are the respective reaction transition states. Clearly, in this model both ES and ESI are productive complexes as it is suggested by the data in Fig. 2. Then the observed velocity is

$$v = v_1 + v_2 \quad (1)$$

where

$$v_1 = k_1[\mathrm{ES}] \quad (2)$$

and

$$v_2 = k_2[\mathrm{ESI}] \quad (3)$$

If we suppose rapid-equilibrium between ES and ESI then the observed velocity can be expressed as

$$v = \left(\frac{k_1 K_i + k_2[I]}{K_i + [I]}\right)[\mathrm{ES}]_T \quad (4)$$

where

$$[\mathrm{ES}]_T = [\mathrm{ES}] + [\mathrm{ESI}] \quad (5)$$

A similar model was successfully used to test the effect of ligands on the unfolding kinetics of barnase [35]. Using the Eyring's formalism for the rate of decomposition of the transition state [36] the kinetic constant of a reaction (assuming a transmission coefficient of 1) can be related to its activation free energy by

$$k = \left(\frac{k_B T}{h}\right) e^{\left(\frac{-\Delta G^{\ddagger}}{RT}\right)} \quad (6)$$

Table 2
Effect of free ADP on the activity of the ADP-dependent enzymes. Results from the global fit to the competitive mechanism of inhibition.

Enzyme	Kinetic parameters[a]		
	k_{cat} s^{-1}	K_M μM	K_I mM
*Ph*PFK	71 ± 1.4	5.8 ± 1.1	3.4 ± 1
*Tl*GK	51 ± 1.4	2.1 ± 0.34	0.30 ± 0.06
*Pf*GK	139 ± 19	4.6 ± 0.72	0.58 ± 0.1

[a] The results shown were derived from a global fit to a competitive inhibition mechanism. Errors are derived from the fitting procedure.

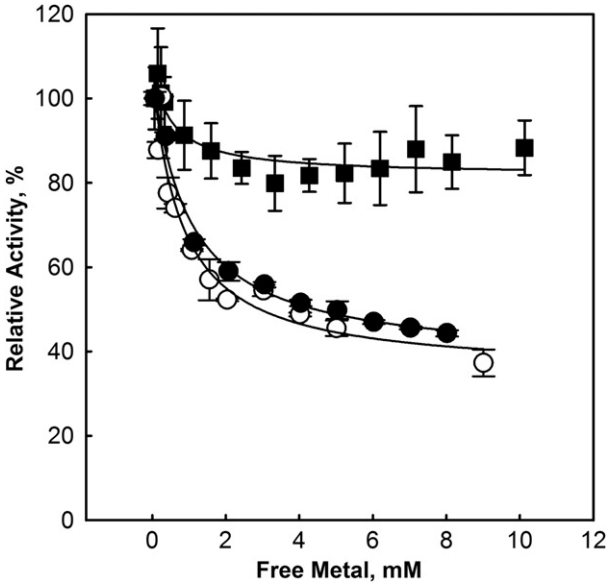

Fig. 2. Effect of free metal concentration on the activity of the ADP-dependent enzymes. The metals assayed were Mg^{2+} for *ph*PFK (squares) and Mn^{2+} for *tl*GK (open circles) and *pf*GK (filled circles). The activity of the enzymes was assayed at saturating MeADP concentrations. The results are shown as relative activity, taking the activity measured at the smallest free metal concentration achieved (68, 82, and 72 μM for *ph*PFK, *tl*GK, and *pf*GK respectively) as 100%. For both glucokinases, the tendency line is the best fit of these data to Eq. (4).

Table 3
Kinetics parameters obtained for the best fitting inhibition models tested on both glucokinases.

Enzyme	Kinetic parameters				
	K_i[a] mM	K_{is}[b] mM	k_{cat}[c] s^{-1}	$k_{cat\text{-}i}$[d] s^{-1}	K_M[e] μM
*tl*GK	1.2 ± 0.3	5.2 ± 0.5	25 ± 0.7	0	11 ± 2
*pf*GK	1.0 ± 0.5	1.0 ± 0.5	255 ± 37	92 ± 8	28 ± 1

[a] Binding to the free protein.
[b] Binding to the MeADP-protein complex.
[c] Catalytic constant of the non-inhibited specie.
[d] Catalytic constant of the inhibited specie.
[e] K_m for the MeADP complex.

where k_B is the Boltzmann constant, h is the Planck constant, T is the temperature, and R the gas constant. Also, considering that

$$\Delta G^{\ddagger} = -RT\ln\left|K^{\ddagger}\right| \quad (7)$$

it is possible to calculate $K_i^{\ddagger}$ from the thermodynamic cycle. Since the model needs a moderately high amount of data, we use the data of Fig. 2 given that these experiments were performed at saturating conditions of substrates and can be used as a very good approximation to k_{cat}.

Using these data we obtained a k_1 (i.e. the step between ES and $E + P$) equal to 51 s^{-1}, k_2 (i.e. the step between ESI and $E + P + I$) 16.6 s^{-1}, K_i 0.79 mM, and $K_i^{\ddagger}$ equal to 2.4 mM for *tl*GK and a k_1 144 s^{-1}, k_2 51 s^{-1}, K_i 0.99 mM, and $K_i^{\ddagger}$ 2.8 mM for *pf*GK. Thus, in both cases the second manganese ion stabilizes the ground state by approximately 0.7 kcal/mol over the transition state, which ultimately results in a diminution of the reaction velocity. Extending the same argument to the rest of the ribokinase superfamily, the regulatory metal should act by modulating the energy difference between the ground and the transition state. In this way, if the second metal binds to the metal-nucleotide complex in a position that reduces the energy difference between the ground and the transition state, it acts as an activator (such as in Pfk-2 [21]), while if it binds in a position that the increase this difference, then it should be act as an inhibitor (such as in this case or for adenosine kinase [20]).

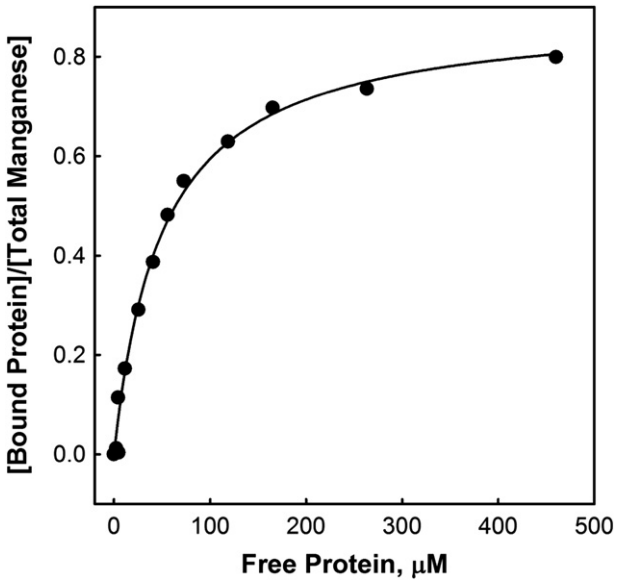

Fig. 3. Binding of Mn^{2+} to the ADP-dependent glucokinase from *T. litoralis* measured by electronic paramagnetic resonance.

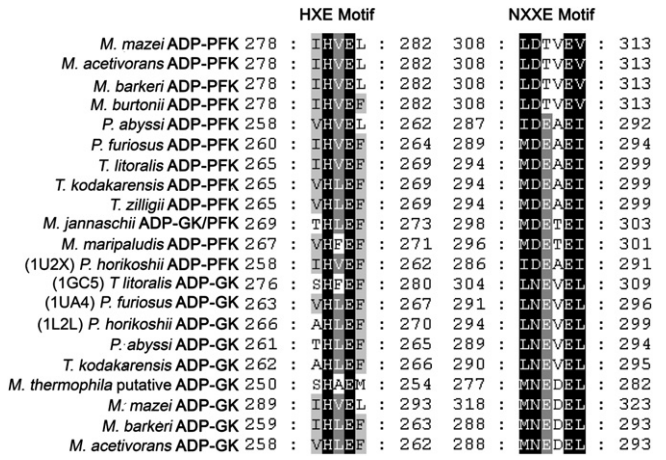

Fig. 4. Multiple sequence alignment of the ADP-dependent sugar kinase family. The two metal binding related motifs HXE and NXXE are shown.

3.3. Molecular dynamics simulations

To explore the microscopic role of divalent metal cations on the ADP-dependent kinases catalytic mechanism we performed molecular dynamics simulations of the *pf*GK and *ph*PFK ternary complexes, in the presence of a magnesium ion located in the NXXE position.

While divalent cations are in general not well simulated by molecular dynamics, for both enzymes the magnesium ion maintains its octahedral coordination geometry throughout the simulation time with no special restrictions, suggesting that the system is well modeled by our approximation. Representative conformations obtained for each simulation are shown in Fig. 5.

In the *pf*GK simulation the magnesium ion is coordinated by 4 water molecules and two oxygen atoms coming from ADP, being one from each phosphate. Due to this bidentate coordination from the nucleotide, the phosphate groups maintain an eclipsed geometry which should help to release the terminal phosphate. In the second coordination sphere are D440 (which is believed to be the general base for catalysis [17]), E295 (from the NXXE motif) and E266, residue which belongs to a highly conserved motif called HXE (Fig. 4). A representative frame is shown in Fig. 5A. The N292 residue (from NXXE) is making a hydrogen bond with the α-phosphate. The distance between the O6 oxygen from glucose and the phosphorous atom from the β-phosphate has an average of 4.9 Å (Fig. 6A) which is similar to the distance seen by x-ray crystallography in other members of the superfamily. Overall, these data suggest that the catalytic ensemble is well modeled by our approximation.

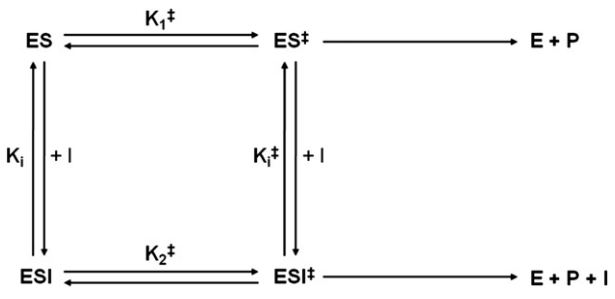

Scheme 1. Schematic representation of the proposed inhibition mechanism.

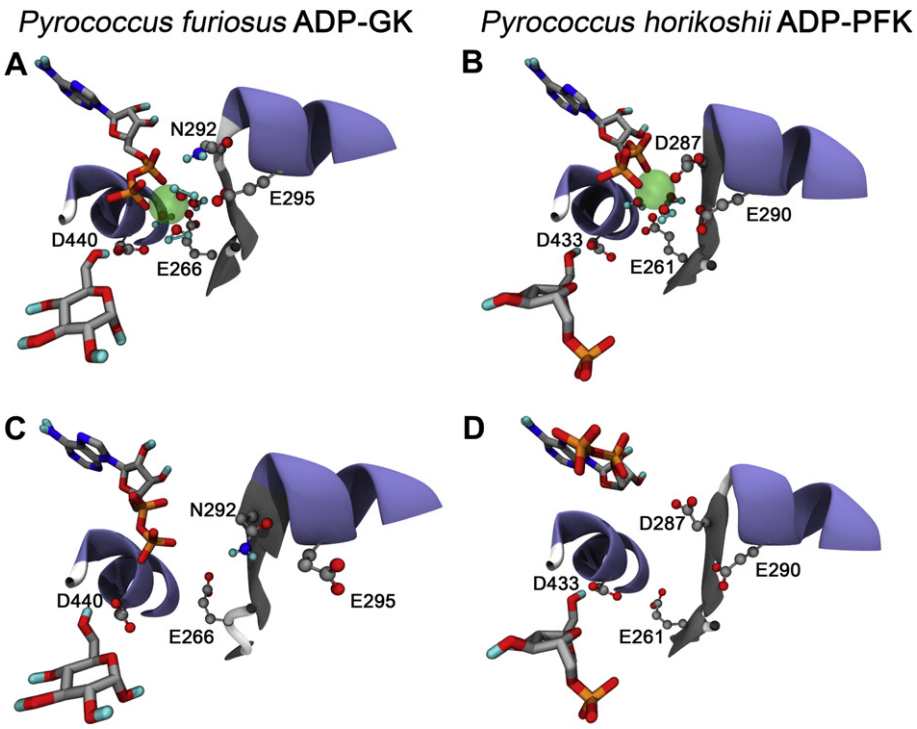

Fig. 5. Representative frames for the ternary complex models obtained through molecular dynamics. A and B show the complexes in the presence of a magnesium ion (*pf*GK and *ph*PFK respectively) while C and D show the complexes in the absence of metal (*pf*GK and *ph*PFK respectively).

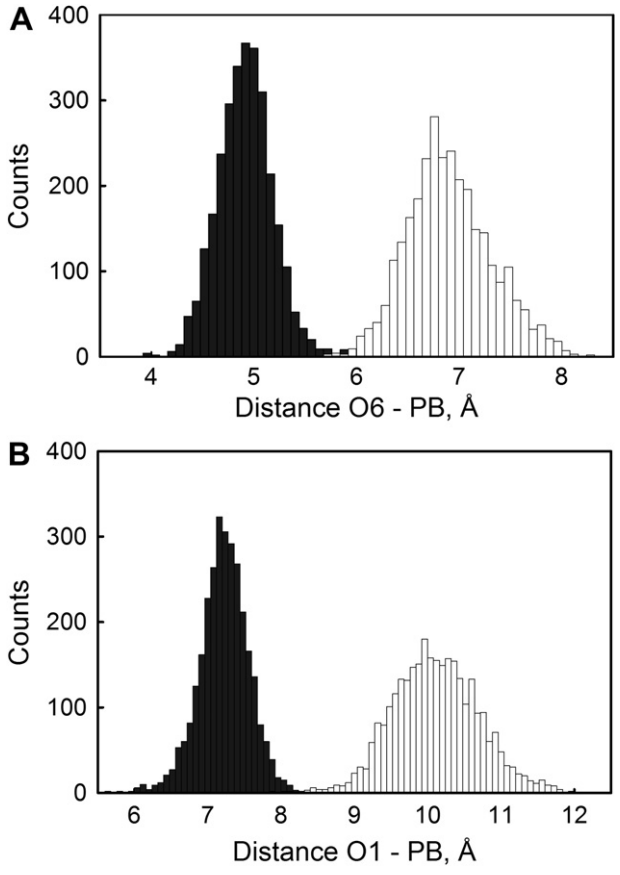

Fig. 6. Donor–acceptor distance histograms for *pf*GK (A) and *ph*PFK (B) obtained through molecular dynamics. In gray are the histograms obtained in presence of metal while in white those in the absence of cation. For *tl*GK the acceptor is O6 and for *ph*PFK is O1. In both cases the donor is the phosphorous atom from the β-phosphate.

To further explore the properties of this ternary complex we calculated the average ion charge density of the trajectory using the APBS software [37]. Surprisingly, it shows a compact region of positive value close to the MeADP complex which could be the regulatory binding site. Fig. 7 shows the average ion charge density of the last 750 ps of simulation. The location of this site suggests that the regulatory metal should be coordinated by the α-phosphate of ADP and the side chain of N196. Also, R194 appears to be somehow related to the hydrogen-bonding network around this site. Interestingly, these two side chains are only conserved in all glucokinases and just the phosphofructokinases from *methanosarcinales* (Fig. 7B). The fact that in *ph*PFK they are a asparagine and a glycine (corresponding to R194 and N196 respectively) could explain the different inhibitory profiles of *tl*GK and *pf*GK with *ph*PFK. Importantly, these two side chains are in the same strand of R197 which has been proven key for the activity of the ADP-dependent enzymes [17,18]. In this way, the binding of an ion to this site should affect the transfer reaction directly.

In *ph*PFK the magnesium ion is coordinated by three water molecules. In this case the fourth molecule seen in *pf*GK is replaced by the side chain of the D287 residue. Interestingly, this corresponds to the asparagine residue of the NXXE motif which is replaced by aspartate in all the ADP-dependent phosphofructokinase sequences (Fig. 4). This could explain the different metal usage profile of phPFK since in this condition the metal binding hole has a higher negative charge density. Noticeably, given that this difference should change drastically the electrostatic potential of the metal-nucleotide binding site it also should affect to regulatory metal binding which also could explain the difference in metal regulation of *ph*PFK respect to *tl*GK or *pf*GK. Altogether, this could reflect a specific metabolic constraint on the ADP-dependent activities which gives biological significance to this cation regulation.

Also, magnesium is coordinated by two oxygen atoms from each phosphate of the nucleotide which produces essentially the same

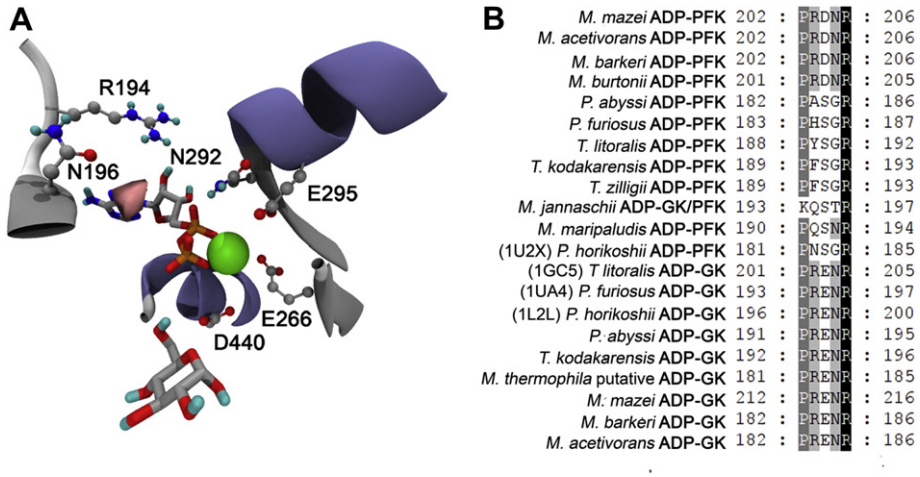

Fig. 7. Analysis of the electrostatic properties of the *pf*GK ternary complex. (A) Average isocontour surface for the ion charge density analysis of the last 750 ps of simulation. The surface corresponding to a value of 0.5 e (electron charge) *M* is shown in pink. (B) A sequence alignment of the residues most likely involved in the coordination of this putative cation binding site. (For interpretation of the references to colour in this figure legend, the reader is referred to the web version of this article.)

geometry as in the *pf*GK case. The distance between the O1 atom from fructose-6-P and the phosphorous atom from the β-phosphate is on average 7.2 Å (Fig. 6B). This value somehow bigger than the expected, could be explained by the fact that in this case, the sugar had to be docked in the active site since to date; there is no empirical structure of an ADP-dependent phosphofructokinase complexed with fructose-6-P. Nevertheless, this docking position has been extensively tested before by mutagenic experiments [18]. In the second coordination sphere are the E290 residue (from NXXE) and the E261 residue (from HXE) (Fig. 5B).

When the magnesium ion is removed from the active site of both proteins, the binding geometry of the nucleotide changes considerably (Fig. 5C and D). In the *pf*GK case, the phosphate tail remains inside the active site, but it twists away from the D440 residue which increases the mean O6-PB distance by 2 Å. This could explain, in part, why it is not possible to transfer the phosphate group in the absence of a divalent metal cation. For *ph*PFK the effect is even bigger. The phosphate tail of the nucleotide is expelled from the active site increasing the mean O1-PB distance by 2.9 Å. Essentially, ADP remains bound to the enzyme mainly through hydrophobic interactions between the adenine group and the protein. The fact that in this condition there is no specific interaction between the phosphates and the protein suggests a big loss in affinity mainly by enthalpic effects which could explains why *ph*PFK has a higher K_i for free ADP than *tl*GK or *pf*GK. Indeed, a very similar conformation is seen in the crystal structure of phPFK bound to AMP [18].

In principle, the data presented in this work suggest that the cation bound to the NXXE motif is mainly related with the catalytic mechanism itself. On the other hand, it remains to be proven by experimental work the predicted location of the second binding site.

4. Conclusions

Several kinds of evidence pointed out that the presence of two metals at the active site may be a general feature of the catalytic mechanism of all the ribokinase family members. Although the ADP-dependent enzymes of the ribokinase superfamily can employ several metals to support enzymatic activity, not all of them have equivalent effects on the regulation of the enzyme activity. In terms of the catalytic metals the three enzymes are quite promiscuous which suggest that the role of these cations is related to the ionic radii and coordination geometry rather than to other specific chemical characteristic. The high K_i values (in the millimolar range) obtained for free ADP inhibition supports the importance of the divalent cation metal for the proper accommodation of the nucleotide in the active site. While some enzymes of the ribokinase superfamily are activated by free divalent metal cations, like Pfk-2 from *E. coli*, others like the ADP-dependent kinases and adenosine kinase are inhibited by them. Here, we proposed a general mechanism for the regulation of the enzymes of this superfamily by metals, where the regulatory metal binds to the transition state and by directly modulating the energy difference between the transition and ground states, acts as an activator or inhibitor.

Acknowledgments

The authors thank to Dr. Mauricio Baez for his guidance in the development of the inhibitory mechanism. We also thank to Dr. Carolina Aliaga (Universidad de Santiago) for the use of the EPR equipment and her support with our experiments. Finally, we are grateful to Dr. Takayoshi Wakagi (University of Tokyo) from whom expression vectors containing both glucokinases were obtained. This work was supported by Fondo Nacional de Desarrollo Científico y Tecnológico (Fondecyt, Chile) Grant 1070111.

References

[1] H. Sakuraba, S. Goda, T. Ohshima, Unique sugar metabolism and novel enzymes of hyperthermophilic archaea, Chem. Rec. 3 (2004) 281–287.
[2] J.E. Tuininga, C.H. Verhees, J. van der Oost, S.W. Kengen, A.J. Stams, W.M. de Vos, Molecular and biochemical characterization of the ADP-dependent phosphofructokinase from the hyperthermophilic archaeon *Pyrococcus furiosus*, J. Biol. Chem. 274 (1999) 21023–21028.
[3] S. Koga, I. Yoshioka, H. Sakuraba, M. Takahashi, S. Sakasegawa, S. Shimizu, T. Ohshima, Biochemical characterization, cloning, and sequencing of ADP-dependent (AMP-forming) glucokinase from two hyperthermophilic archaea, *Pyrococcus furiosus* and *Thermococcus litoralis*, J. Biochem. 128 (6) (2000) 1079–1085.
[4] C.H. Verhees, J.E. Tuininga, S.W. Kengen, A.J. Stams, J. van der Oost, W.M. de Vos, ADP-dependent phosphofructokinases in mesophilic and thermophilic methanogenic archaea, J. Bacteriol. 183 (24) (2001) 7145–7153.
[5] R.S. Ronimus, J. Koning, H.W. Morgan, Purification and characterization of an ADP-dependent phosphofructokinase from *Thermococcus zilligii*, Extremophiles 3 (2) (1999) 121–129.
[6] R.S. Ronimus, H.W. Morgan, Cloning and biochemical characterization of a novel mouse ADP-dependent glucokinase, Biochem. Biophys. Res. Commun. 315 (3) (2004) 652–658.
[7] S. Ito, S. Fushinobu, I. Yoshioka, S. Koga, H. Matsuzawa, T. Wakagi, Structural basis for the ADP-specificity of a novel glucokinase from a hyperthermophilic archaeon, Structure 9 (3) (2001) 205–214.

[8] P. Bork, C. Sander, A. Valencia, Convergent evolution of similar enzymatic function on different protein folds: the hexokinase, ribokinase, and galactokinase families of sugar kinases, Protein Sci. 2 (1) (1993) 31–40.
[9] Y. Zhang, M. Dougherty, D.M. Downs, S.E. Ealick, Crystal structure of an aminoimidazole riboside kinase from *Salmonella enterica*: implications for the evolution of the ribokinase superfamily, Structure 12 (10) (2004) 1809–1821.
[10] V. Guixé, F. Merino, The ADP-dependent sugar kinase family: kinetic and evolutionary aspects, IUBMB Life 61 (7) (2009) 753–761.
[11] J.C. Torres, V. Guixé, J. Babul, A mutant phosphofructokinase produces a futile cycle during gluconeogenesis in *Escherichia coli*, Biochem. J. 327 (1997) 675–684.
[12] M.C. Maj, B. Singh, R.S. Gupta, Structure-activity studies on mammalian adenosine kinase, Biochem. Biophys. Res. Commun. 275 (2) (2000) 386–393.
[13] I.I. Mathews, M.D. Erion, S.E. Ealick, Structure of human adenosine kinase at 1.5 Å resolution, Biochemistry 37 (45) (1998) 15607–15620.
[14] J.A. Sigrell, A.D. Cameron, T.A. Jones, S.L. Mowbray, Structure of *Escherichia coli* ribokinase in complex with ribose and dinucleotide determined to 1.8 Å resolution: insights into a new family of kinase structures, Structure 6 (2) (1998) 183–193.
[15] M.A. Schumacher, D.M. Scott, I.I. Mathews, S.E. Ealick, D.S. Roos, B. Ullman, R.G. Brennan, Crystal structures of *Toxoplasma gondii* adenosine kinase reveal a novel catalytic mechanism and prodrug binding, J. Mol. Biol. 298 (5) (2000) 875–893.
[16] N. Campobasso, I.I. Mathews, T.P. Begley, S.E. Ealick, Crystal structure of 4-methyl-5-beta-hydroxyethylthiazole kinase from *Bacillus subtilis* at 1.5 Å resolution, Biochemistry 39 (27) (2000) 7868–7877.
[17] S. Ito, S. Fushinobu, J.J. Jeong, I. Yoshioka, S. Koga, H. Shoun, T. Wakagi, Crystal structure of an ADP-dependent glucokinase from *Pyrococcus furiosus*: implications for a sugar induced conformational change in ADP-dependent kinase, J. Mol. Biol. 331 (4) (2003) 871–883.
[18] M.A. Currie, F. Merino, T. Skarina, A.H.Y. Wong, A. Singer, G. Brown, A. Savchenko, A. Caniuguir, V. Guixé, A.F. Yakunin, Z. Jia, ADPdependent 6-phosphofructokinase from *Pyrococcus horikoshii* OT3: structure determination and biochemical characterization of PH1645, J. Biol. Chem. 284 (34) (2009) 22664–22671.
[19] R. Cabrera, J. Babul, V. Guixé, Ribokinase family evolution and the role of conserved residues at the active site of the PfkB subfamily representative, Pfk-2 from *Escherichia coli*, Arch. Biochem. Biophys. 502 (1) (2010) 23–30.
[20] M.C. Maj, B. Singh, R.S. Gupta, Pentavalent ions dependency is a conserved property of adenosine kinase from diverse sources: identification of a novel motif implicated in phosphate and magnesium ion binding and substrate inhibition, Biochemistry 41 (12) (2002) 4059–4069.
[21] R.E. Parducci, R. Cabrera, M. Baez, V. Guixé, Evidence for a catalytic Mg^{2+} ion and effect of phosphate on the activity of *Escherichia coli* phosphofructokinase-2: regulatory properties of a ribokinase family member, Biochemistry 45 (30) (2006) 9291–9299.
[22] M. Li, F. Kwok, W. Chang, C. Lau, J. Zhang, S.C.L. Lo, T. Jiang, D. Liang, Crystal structure of brain pyridoxal kinase, a novel member of the ribokinase superfamily, J. Biol. Chem. 277 (48) (2002) 46385–46390.
[23] L. Miallau, W.N. Hunter, S.M. McSweeney, G.A. Leonard, Structures of *Staphylococcus aureus* d-tagatose-6-phosphate kinase implicate domain motions in specificity and mechanism, J. Biol. Chem. 282 (27) (2007) 19948–19957.
[24] R. Cabrera, A.L.B. Ambrosio, R.C. Garratt, V. Guixé, J. Babul, Crystallographic structure of phosphofructokinase-2 from *Escherichia coli* in complex with two ATP molecules. Implications for substrate inhibition, J. Mol. Biol. 383 (3) (2008) 588–602.
[25] J.A. Rivas-Pardo, A. Caniuguir, C.A.M. Wilson, J. Babul, V. Guixé, Divalent metal cation requirements of phosphofructokinase-2 from *E. coli*: evidence for a high affinity binding site for Mn^{2+}, Arch. Biochem. Biophys. 505 (1) (2011) 60–66.
[26] H. Tsuge, H. Sakuraba, T. Kobe, A. Kujime, N. Katunuma, T. Ohshima, Crystal structure of the ADP-dependent glucokinase from *Pyrococcus horikoshii* at 2.0-Å resolution: a large conformational change in ADP-dependent glucokinase, Protein Sci. 11 (10) (2002) 2456–2463.
[27] A. Kornberg, W.E. Pricer, Enzymatic esterification of alpha-glycerophosphate by long chain fatty acids, J. Biol. Chem. 204 (1953) 345–357.
[28] J.C. Phillips, R. Braun, W. Wang, J. Gumbart, E. Tajkhorshid, E. Villa, C. Chipot, R.D. Skeel, L. Kale, K. Schulten, Scalable molecular dynamics with NAMD, J. Comput. Chem. 26 (16) (2005) 1781–1802.
[29] A. MacKerell Jr., D. Bashford, M. Bellott, R. Dunbrack Jr., J. Evanseck, M. Field, S. Fischer, J. Gao, H. Guo, S. Ha, D. Joseph-McCarthy, L. Kuchnir, K. Kuczera, F.T.K. Lau, C. Mattos, S. Michnick, T. Ngo, D.T. Nguyen, B. Prodhom, W.E. Reiherand, B. Roux, M. Schlenkrich, J.C. Smith, R. Stote, J. Straub, M. Watanabe, J. Wiorkiewicz-Kuczera, D. Yin, M. Karplus, All-atom empirical potential for molecular modeling and dynamics studies of proteins, J. Phys. Chem. B 102 (18) (1998) 3586–3616.
[30] F. Merino, V. Guixe, Specificity evolution of the ADP-dependent sugar kinase family: *in silico* studies of the glucokinase/phosphofructokinase bifunctional enzyme from *Methanocaldococcus jannaschii*, FEBS J. 275 (16) (2008) 4033–4044.
[31] W. Humphrey, A. Dalke, K. Schulten, VMD: visual molecular dynamics, J. Mol. Graph. 14 (1) (1996) 33–38.
[32] C. Andreini, I. Bertini, G. Cavallaro, G.L. Holliday, J.M. Thornton, Metal ions in biological catalysis: from enzyme databases to general principles, J. Biol. Inorg. Chem. 13 (8) (2008) 1205–1218.
[33] M.E. Maguire, J.A. Cowan, Magnesium chemistry and biochemistry, Biometals 15 (3) (2002) 203–210.
[34] V. Guixe, J. Babul, Effect of ATP on phosphofructokinase-2 from *Escherichia coli*. A mutant enzyme altered in the allosteric site for MgATP, J. Biol. Chem. 260 (20) (1985) 11001–11005.
[35] J. Sancho, E.M. Meiering, A.R. Fersht, Mapping transition states of protein unfolding by protein engineering of ligand-binding sites, J. Mol. Biol. 221 (3) (1991) 1007–1014.
[36] H. Eyring, The activated complex in chemical reactions, J. Chem. Phys. 3 (1935) 107–115.
[37] N.A. Baker, D. Sept, S. Joseph, M.J. Holst, J.A. McCammon, Electrostatics of nanosystems: application to microtubules and the ribosome, Proc. Natl. Acad. Sci. U S A 98 (18) (2001) 10037–10041.